

Neural Network based Formation of Cognitive Maps of Semantic Spaces and the Emergence of Abstract Concepts

Paul Stoewer^{1,2}, Achim Schilling^{1,3}, Andreas Maier², and Patrick Krauss^{1,2,3,4,*}

¹Cognitive Computational Neuroscience Group, University Erlangen-Nuremberg, Germany

²Pattern Recognition Lab, University Erlangen-Nuremberg, Germany

³Neuroscience Lab, University Hospital Erlangen, Germany

⁴Linguistics Lab, University Erlangen-Nuremberg, Germany

*corresponding author

October 31, 2022

Keywords:

cognitive maps, semantic space, multi-scale successor representations, hippocampus, entorhinal cortex, navigation, memory, linguistic constructions, mental space, neural networks, artificial intelligence

Abstract

How do we make sense of the input from our sensory organs, and put the perceived information into context of our past experiences? The hippocampal-entorhinal complex plays a major role in the organization of memory and thought. The formation of and navigation in cognitive maps of arbitrary mental spaces via place and grid cells can serve as a representation of memories and experiences and their relations to each other. The multi-scale successor representation is proposed to be the mathematical principle underlying place and grid cell computations. Here, we present a neural network, which learns a cognitive map of a semantic space based on 32 different animal species encoded as feature vectors. The neural network successfully learns the similarities between different animal species, and constructs a cognitive map of 'animal space' based on the principle of successor representations with an accuracy of around 30% which is near to the theoretical maximum regarding the fact that all animal species have more than one possible successor, i.e. nearest neighbor in feature space. Furthermore, a hierarchical structure, i.e. different scales of cognitive maps, can be modeled based on multi-scale successor representations. We find that, in fine-grained cognitive maps, the animal vectors are evenly distributed in feature space. In contrast, in coarse-grained maps, animal vectors are highly clustered according to their biological class, i.e. amphibians, mammals and insects. This could be a possible mechanism explaining the emergence of new abstract semantic concepts. Finally, even completely new or incomplete input can be represented by interpolation of the representations from the cognitive map with remarkable high accuracy of up to 95%. We conclude that the successor representation can serve as a weighted pointer to past memories and experiences, and may therefore be a crucial building block to include prior knowledge, and to derive context knowledge from novel input. Thus, our model provides a new tool to complement contemporary deep learning approaches on the road towards artificial general intelligence.

Introduction

The hippocampal-entorhinal complex supports spatial navigation and forms cognitive maps of the environment [1]. However, recent research suggests that formation of and navigation on cognitive maps are not limited to physical space, but extend to more abstract conceptual, visual or even social spaces [2–4]. A simplified processing framework for the complex can be described as following: highly processed information from our sensory organs are fed into the hippocampal complex where the perceived information is put into context, i.e. associated with past experiences [5]. Grid [6] and place [7] cells enable map like codes, and research suggests that they form cognitive maps [8] [9], thereby contributing to process memories, emotions and navigation [10](cf. 1).

Furthermore, it is known that the hippocampus plays a crucial role for episodic and declarative memory [11, 12]. However, whether memories are directly stored in the hippocampus, and how they are retrieved through the hippocampus, is depending on different theories still under discussion. Therefore, the exact role of the hippocampus in the domain of memory is still not fully understood [13]. According to the *multiple trace theory* [14], memories are not directly stored in the hippocampus. Instead, memory content is stored in the cerebral cortex, and the hippocampus forms representations of memory traces which can serve as pointers to retrieve memory content from the cerebral cortex.

Furthermore memory can be represented at different scales along the hippocampal longitude axis, like e.g. varying spatial resolutions [15]. In the context of spatial navigation the different scales serve to navigate with different horizons [16]. In the context of abstract conceptual spaces, different scales might correspond to different degrees of abstraction [17]. In general, multi-scale cognitive maps enable flexible planning, generalization and detailed representation of information [18].

Various different computational models try to explain the versatility of the hippocampal-entorhinal complex. One of these candidate models successfully reproduces the firing patterns of place and grid cells in a large number of different experimental scenarios, indicating that the hippocampus works like a predictive map based on multi-scale successor representations (SR) [19–21].

In a previous study, we introduced a neural network based implementation of this framework, and demonstrated its applicability to several spatial navigation and non-spatial linguistic tasks [22]. Here, we further extended our model as shown in Figure 1. In particular, we build a neural network which learns the SR for a non-spatial navigation task based on input feature vectors representing different animal species. The semantic feature vectors represent memory traces, and therefore combine the memory trace theory with the cognitive map theory.

Methods

Successor Representation

The developed cognitive map is based on the principle of the successor representation (SR). As proposed by Stachenfeld and coworkers the SR can model the firing patterns of the place cells in the hippocampus [20]. The SR was originally designed to build a representation of all possible future rewards $V(s)$ that may be achieved from each state s within the state space over time [23]. The future reward matrix $V(s)$ can be calculated for every state in the environment, whereas the parameter t indicates the number of time steps in the future that are taken into account, and $R(s_t)$ is the reward for state s at time t . The discount factor $\gamma[0, 1]$ reduces the relevance of states s_t that are further in the future relative to the respective initial state s_0 (cf. eq. 1).

$$V(s) = E\left[\sum_{t=0}^{\infty} \gamma^t R(s_t) | s_0 = s\right] \quad (1)$$

Here, $E[\]$ denotes the expectation value.

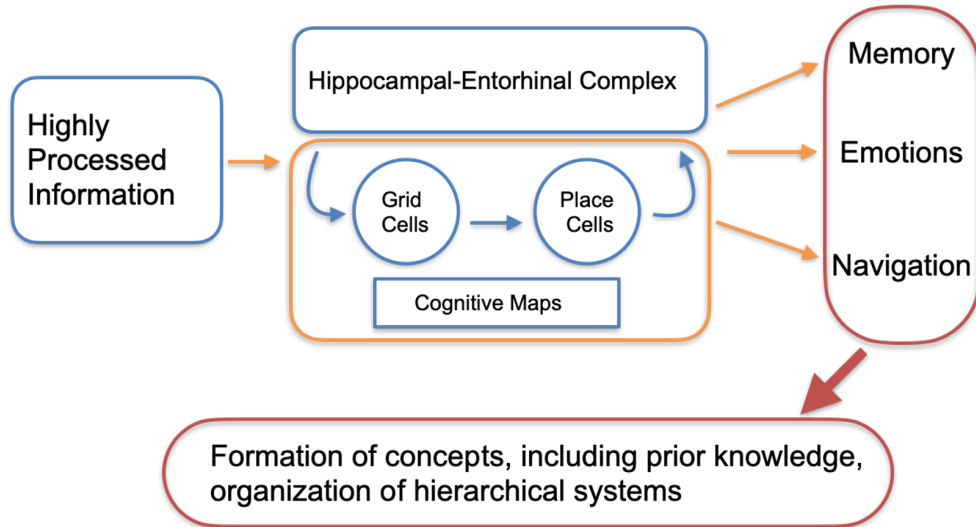


Figure 1: **Simplified sketch model of the hippocampal-entorhinal complex.** Highly processed information is fed into the system and becomes associated with existing memories and past experiences. Place and grid cells enable the formation of map like codes, and finally cognitive maps. The complex also supports navigation, emotions, the formation of concepts, inclusion of prior knowledge, and the organization of hierarchical representations.

The future reward matrix $V(s)$ can be re-factorized using the SR matrix M , which can be computed from the state transition probability matrix T of successive states (cf. eq. 2). In case of supervised learning, the environments used for our model operate without specific rewards for each state. For the calculation of these SR we set $R(s_t) = 1$ for every state.

$$V(s) = \sum_{s'} M(s, s') R(s') \quad M = \sum_{t=0}^{\infty} \gamma^t T^t \quad (2)$$

Animal Data Set

The construction of the cognitive map is based on a data set which quantifies seven different semantic features of 32 animal species (Table 1). The corresponding test data set is shown in Table 2.

The data matrix represents the memory matrix $M(m)$, which our cognitive map is based on. Therefore every animal represents a past memory, and reflects a state in our model. To use the matrix for our supervised learning approach, we need to sample successor labels for every state, which reflect the similarity between animal species. We choose to use the Euclidean distance to calculate the transition probabilities for our state space. Therefore animal species sharing similar semantic features have a higher state transition probability.

$$T(s, s') = \frac{1}{\|m_s - m_{s'}\|} \quad (3)$$

For the generation of the training and test data set, a random starting state is chosen and also a random probability ranging from 0 to 1 is sampled. The input feature vector for the chosen input state is altered by a random range of 0 to 15% to make the training more robust to novel inputs. Based on the sampled probability and the cumulative density function of the defined successor representation matrix, a valid successor state is randomly drawn as label. 10% of the generated samples are not used for training, but are instead preserved as validation data set.

Name	Height(cm)	Weight(kg)	Number Legs	Danger(subjective)	Reproduction (2=Birth, 1= Eggs)	Fur(2=No,1=Yes)	Lungs(2=No,1=Yes)
Elephant	350	6000	4	60	2	2	1
Tiger	100	100	4	100	2	1	1
Lion	120	175	4	100	2	1	1
Dog	70	30	4	20	2	1	1
Rabbit	40	2	4	0	2	1	1
Bear	200	500	4	60	2	1	1
Cow	120	500	4	20	2	1	1
Deer	70	20	4	0	2	1	1
Cat	30	4	4	5	2	1	1
Beaver	60	25	4	5	2	1	1
Giraffe	500	1200	4	40	2	1	1
Ape	70	40	4	30	2	1	1
Horse	120	250	4	10	2	1	1
Camel	125	400	4	10	2	1	1
Goat	70	60	4	5	2	1	1
Sheep	60	20	4	5	2	1	1
Pig	60	200	4	5	2	2	1
Hamster	5	0.2	4	0	2	1	1
Dolphine	200	60	0	10	2	2	1
Raccoon	50	15	4	5	2	1	1
Red Pander	30	5	4	5	2	1	1
Ant	0,1	0,00001	6	1	1	2	2
Bee	1	0,0001	6	5	1	2	2
Cockroach	5	0,005	6	0	1	2	2
Goliathus	8	5	6	0	1	2	2
Giant weta	10	0,035	6	0	1	2	2
Heteropteryx	15	0,05	6	0	1	2	2
Cane toad	15	1	4	0	1	2	1
Fire Salamander	17	0,035	4	0	1	2	1
Frog	4	0,01	4	0	1	2	1
Olm	20	0,02	4	0	1	2	1
Tree Frog	4	0,005	4	0	1	2	1

Table 1: **Training data set used to create the cognitive room.** It consists of 32 different animal species, which belong to three different taxonomic classes: mammals, insects and amphibians. Each animal is characterized by seven semantic features: Height, weight, number of legs, its danger level, the reproduction system, if it has fur and if it has lungs.

Name	Height(cm)	Weight(kg)	Number Legs	Danger(subjective)	Reproduction (2=Birth, 1= Eggs)	Fur(2=No,1=Yes)	Lungs(2=No,1=Yes)
Jaguar	70	70	4	90	2	1	1
Donkey	100	200	4	10	2	1	1
Wild boar	70	180	4	20	2	1	1
Melontha	2,5	0,001	6	0	1	2	2
Dragonfly	6	0,0003	6	0	1	2	2
Wasp	1,5	0,00008	6	20	1	2	2

Table 2: **Test data used to evaluate the interpolation capabilities of the trained neural network.** It consists of 6 different animal species, which belong to three different taxonomic classes: mammals, insects and amphibians. Again, each animal is characterized by seven semantic features: Height, weight, number of legs, its danger level, the reproduction system, if it has fur and if it has lungs.

Neural network architectures and training parameters

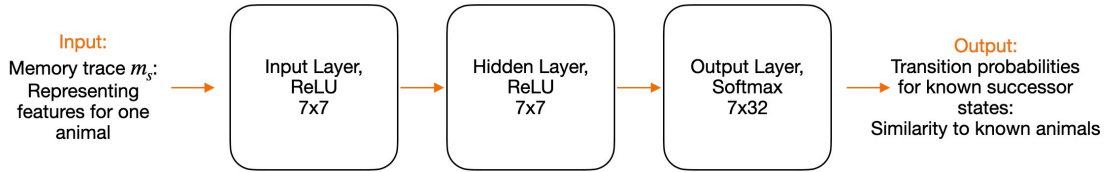


Figure 2: **Architecture of the trained neural network.** The network receives a memory trace of animal features as input. The size of the input and hidden layer is equal to the number of features in the input. The output layer is a softmax layer with 32 neurons, matching the number of memory traces in the training memory matrix. The output of the network is the probability of the similarity of the input to the entries of the memory matrix used during training.

We set up a three-layered feed forward neural network. The network consists of 7 input neurons and has 7 neurons in the hidden layer. Both use a ReLU activation function. The output layer consists of 32 neurons with a softmax activation function (cf. 2). The network learns the transition probabilities of the environment, i.e. in our case the memory space. Smaller number of neurons in the hidden layer did not influence the results in previous experiments [22]. We trained three networks for different discount factors of the successor representation, with $\gamma = (0.3, 0.7, 1.0)$ and $t = 10$. Note that, larger discount factors correspond to a larger time horizon, i.e. taking into account more future steps. The networks were trained for 500 epochs, with a batch size of 50, 50000 training samples, using the Adam optimizer with a learning rate of 0.001 and categorical cross-entropy as loss function.

Transition probability and successor representation matrix

After the training process, the networks can predict all probabilities for the successor states for any given input feature vector. Concatenating the predictions of all known animal states leads to the successor representation matrix of the cognitive room. The output of the network is a vector shaped like a row of the respective environment’s SR matrix and can therefore directly be used to fill the SR matrix, respectively.

Interpolating unknown features

We propose that the successor representation can be used as a pointer to stored memories. In our case we have the saved memories of 32 animal species in the memory trace matrix which we use for training the network. If incomplete information is fed into the network (unknown values set to -1 in the input feature vector), it still outputs predictions for the possible transition probabilities.

$$m_{interpolated} = SR_{prediction} * M(m_s) \quad (4)$$

Thus, we can use the prediction from the network, and perform a matrix multiplication with our known memory matrix in order to derive an interpolated feature vector for the incomplete or unknown input (cf. 4).

Multi-dimensional scaling

A frequently used method to generate low-dimensional embeddings of high-dimensional data is t-distributed stochastic neighbor embedding (t-SNE) [24]. However, in t-SNE the resulting low-dimensional projections can be highly dependent on the detailed parameter settings [25], sensitive

to noise, and may not preserve, but rather often scramble the global structure in data [26, 27]. In contrast to that, multi-Dimensional-Scaling (MDS) [28–31] is an efficient embedding technique to visualize high-dimensional point clouds by projecting them onto a 2-dimensional plane. Furthermore, MDS has the decisive advantage that it is parameter-free and all mutual distances of the points are preserved, thereby conserving both the global and local structure of the underlying data.

When interpreting patterns as points in high-dimensional space and dissimilarities between patterns as distances between corresponding points, MDS is an elegant method to visualize high-dimensional data. By color-coding each projected data point of a data set according to its label, the representation of the data can be visualized as a set of point clusters. For instance, MDS has already been applied to visualize for instance word class distributions of different linguistic corpora [32], hidden layer representations (embeddings) of artificial neural networks [33, 34], structure and dynamics of recurrent neural networks [35–37], or brain activity patterns assessed during e.g. pure tone or speech perception [32, 38], or even during sleep [39, 40]. In all these cases the apparent compactness and mutual overlap of the point clusters permits a qualitative assessment of how well the different classes separate.

Code Implementation

The models were coded in Python 3.10. The neural networks were design using the Keras [41] library with TensorFlow [42]. Mathematical operations were performed with numpy [43] and scikit-learn [44] libraries. Visualizations were realised with matplotlib [45].

Results

Learning structures by observing states and their successors

The models were trained to learn the underlying structure of the data set. In particular, we trained three different neural networks using different discount factors ($\gamma = (0.3, 0.7, 1.0)$, $t = 10$). The resulting successor representation matrices for each parameter setting are very similar to the ground truth (Figure 3), and the corresponding root-mean-squared errors (RMSE) are extremely low: 0.02034 for $\gamma = 0.3$ (Figure 3a), 0.01496 for $\gamma/0.7$ (Figure 3b), and 0.00854 for $\gamma = 1.0$ (Figure 3c).

The accuracy for the model with the discount factor $\gamma = 0.3$ increased quickly during the first 100 epochs, and then slowly continued to increase until the end of training at epoch 500 where the highest accuracy of 60% was achieved (Figure 4a).

In contrast, the training procedure quickly reached a saturation of the accuracy for the two models with discount factors $\gamma = 0.7$ and $\gamma = 1.0$ after around 200 epochs, with maximum training and validation accuracies of approximately 30% or 35% respectively (Figure 4b, c).

Scaling of cognitive maps depends on discount factor of successor representation

The discount factor of the SR is proposed to enable scaling of the cognitive maps, and thus to represent hierarchical structures, similar to the different mesh sizes of grid cells along the longitudinal axis of the hippocampus and the entorhinal cortex [20]. Actually, memory representations, such as the internal representation of space, systematically vary in scale along the hippocampal long axis [15]. This scaling has been suggested to be used for targeted navigation with different horizons [16] or even for encoding information from smaller episodes or single objects to more complex concepts [17].

In order to visualize the learned SR underlying the cognitive maps, we calculate MDS pojections from the SR matrices (Figure 5). Furthermore, as an estimate for the map scaling, we calculate the general discrimination value (GDV, cf. Methods) for each map.

We find that the resulting scaling of the cognitive maps depends on the discount factor of the underlying SR matrix, and that the GDV correlates with the discount factor. A small discount

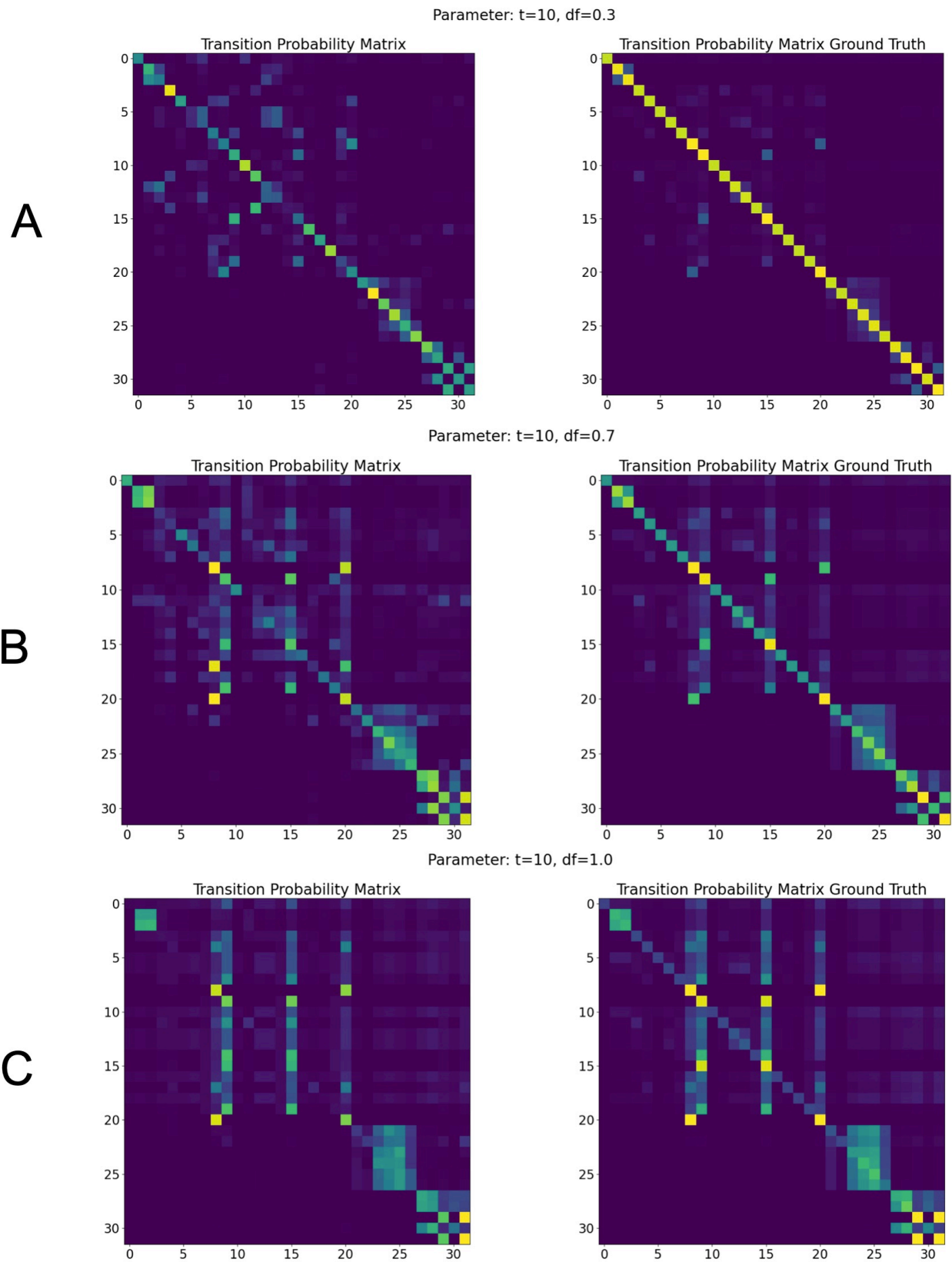


Figure 3: **Learned successor representation (SR) matrices and corresponding ground truths.** Learned SR matrices (left column) are very similar to their corresponding ground truth SR matrices (right column). a: For a discount factor of $\gamma = 0.3$, the RMSE between learned and ground truth SR matrix is 0.02034. b: For $\gamma = 0.7$, the RSME is 0.01496. c: For $\gamma = 1.0$, the RMSE is 0.00854.

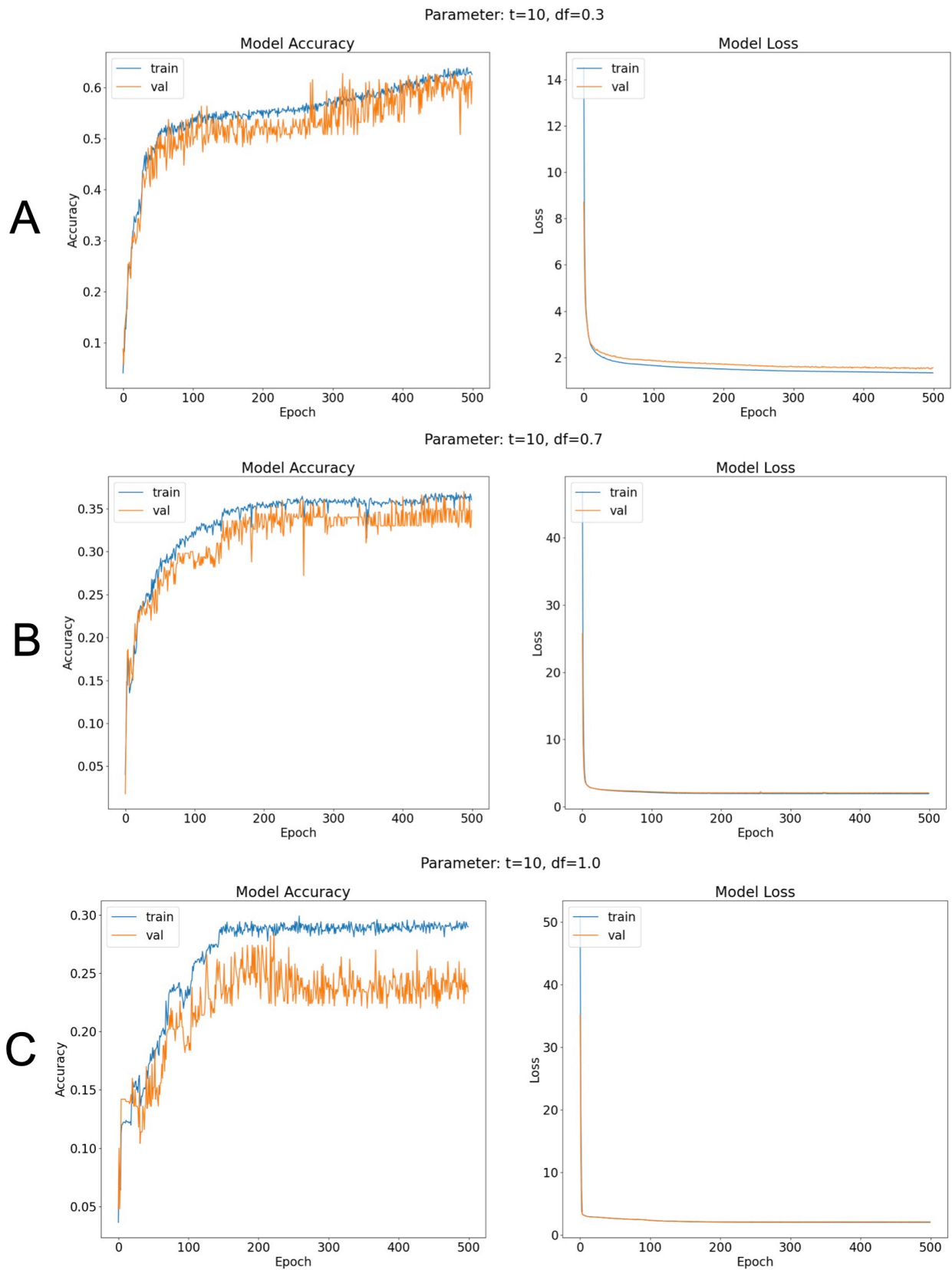


Figure 4: **Accuracies and loss for different models.** Training accuracies (blue) and validation accuracies (orange) during training are shown in the left column. The corresponding loss is shown in the right column. a: For a discount factor of $\gamma = 0.3$, the highest accuracy of 60% was achieved. b: For $\gamma = 0.7$, the accuracy saturates after 200 epochs at 30%. c: For $\gamma = 1.0$, the accuracy saturates after 200 epochs at 35%.

factor of $\gamma = 0.3$ results in a fine-grained and detailed cognitive map where each object is clearly separated from the others, and similar objects, i.e. animal species, are closer together (Figure 5a). With a GDV of -0.322 , the clustering is relatively low compared to the other maps. This cognitive map resembles so called self-organizing maps introduced by Kohonen [46], and might correspond to word fields proposed in linguistics [47].

A discount factor $\gamma = 0.7$ results in an intermediate scale cognitive map with a GDV of -0.355 (Figure 5b).

Finally, a discount factor of $\gamma = 1.0$ results in the most course-grained cognitive map. Here, individual animal species are no longer clearly separated from each other, but are forming instead representational clusters that correspond to taxonomic animal classes, i.e. mammals, insects and amphibians (Figure 5c). Consequently, this map has the lowest GDV of -0.403 , indicating the best clustering. This type of representation generalizing from individual objects might correspond to the emergence of cognitive categories, as suggested e.g. in prototype semantics [48].

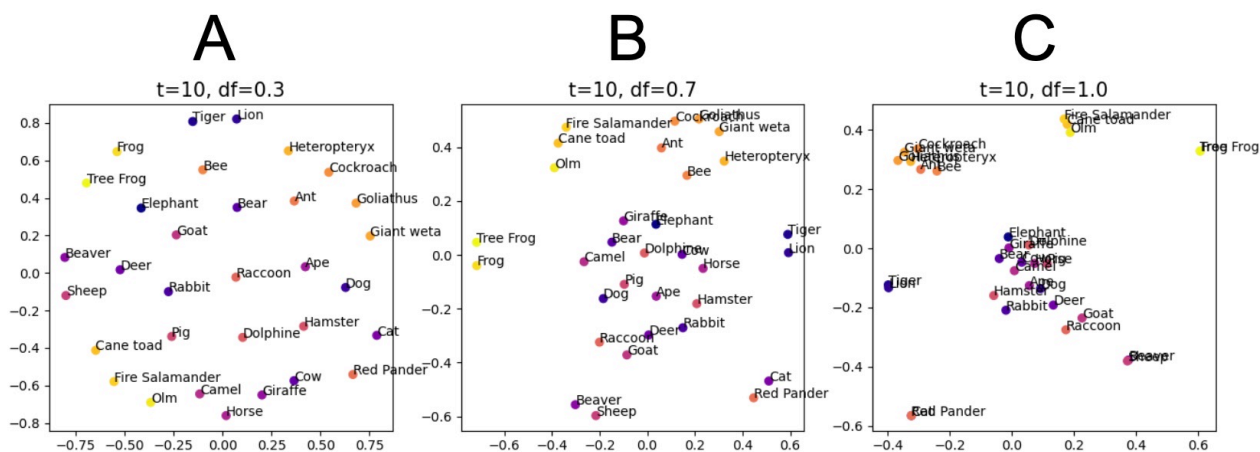


Figure 5: **Different scalings of cognitive maps.** Shown are MDS projections of SR matrices with different discount factors γ . a: For a low discount factor $\gamma = 0.3$, the resulting map is most fine-grained and detailed with little clustering (GDV: -0.322). b: A medium discount factor of $\gamma = 0.7$ results in an intermediate scale with more clustering (GDV: -0.355) compared to (a). c: The largest discount factor $\gamma = 1.0$ results in the most coarse-grained map. Here, individual animal species are no longer distinguishable, but instead form different clusters corresponding to more abstract concepts, i.e. the taxonomic animal classes mammals (blue, purple), insects (orange), and amphibians (yellow) (GDV: -0.403). Note that, a GDV of -1.0 indicates perfect clustering, whereas a GDV of 0.0 indicates no clustering at all.

Feature inference for incomplete feature vectors

The neural network which learned the structure of the input data successfully can now be used to interact with unseen data. The prediction of the trained neural network can be used as weighted pointer to the memorized objects (animal species) in the training data set. The vector of a previous unseen animal, the *jaguar*, is feed into the network for prediction 6. Three features (danger, fur, lungs) are missing, i.e. are set to -1 . The binary features are predicted well independent from the discount factor. The 'danger' feature is inferred best for the smallest discount factor $\gamma = 0.3$. Note that, also the not missing parameters are changed by the prediction. In general, larger discount factors better infer more general features, whereas smaller discount factors better infer more specific features.

We further evaluated the model with our interpolation test data set (cf. 2). We trained ten models with the parameters $\gamma = 1.0$ and $t = 10$. In Figure 7 the distances of the predictions of

different features in comparison to the ground truth is summarized. The percentage is based on the maximum distance of the according feature. The evaluation is plotted for the feature vectors, with up to 6 missing entries for every prediction. The distance of the prediction to ground truth with no missing entries is in general low ranging from around 5% to 25% (corresponding to 95% to 75% accuracy), indicating high similarity. However, dissimilarity increases to 40% in case of 6 missing features. The distance is however different for each feature. While the semantic feature 'number of legs' is predicted well, the height of the animal is predicted with less accuracy. Furthermore, the variance differs for different models. Especially the badly predicted predicted features like 'height' and 'weight' the variance is quite large.

Height	Weight	#Legs	Danger	Rep.	Fur	Lungs
70	70	4	90(-1)	2	1(-1)	1(-1)



γ	Height	Weight	#Legs	Danger	Rep.	Fur	Lungs
0.3	109.35	161.53	4.001	80.02	1.99	1.01	1.002
0.7	62.01	48.14	4.006	4.54	1.94	1.06	1.01
1.0	56.35	21.51	4.006	4.97	1.97	1.002	1.003

Figure 6: **Interpolation of the test data set feature vector 'Jaguar'**. Three semantic features (dangerous, having a fur and having lungs) are missing, i.e. are replaced by the value -1 . The three networks trained with different discount factors $\gamma = (0.3, 0.7, 1.0)$ infer the missing features. Binary semantic features are inferred well in all cases. The 'dangerous' feature is badly predicted for large discount factors $\gamma = (0.7, 1.0)$. In contrast, in case of the lower discount factor $\gamma = 0.3$, it is predicted well.

Discussion

In this study we have demonstrated that arbitrary feature spaces can be learned efficiently on the basis of successor representations with neural networks. In particular, the networks learn a representation of the semantic feature space of animal species as a cognitive map. The network achieves an accuracy of around 30% which is near to the theoretical maximum regarding the fact that all animal species have more than one possible successor, i.e. nearest neighbor in feature space. Our approach therefore combines the concepts of feature space and state space. The emerging representations therefore resemble the proposed general and abstract cognitive maps described by Bellmund et al. [49].

Our model extends our past work, where we reproduced place cell fire patterns in a spatial navigation and a non-spatial linguistic task based on the successor representation [22]. The innovation of our here presented approach is, that we can use the successor representation with arbitrary new

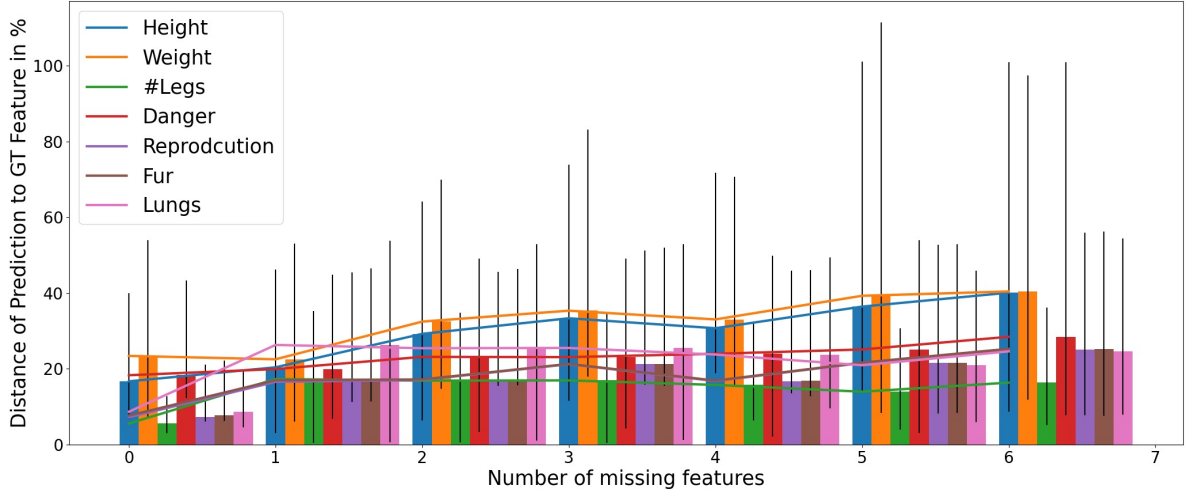


Figure 7: **Dissimilarities between interpolated features and ground truth.** 10 networks with $\gamma = 1.0$ have been trained. Dissimilarity is low in case of a no or a single missing feature, and increases with number of missing features up to 40% for six missing features. In general, binary semantic features are inferred with better accuracy than non-binary semantic features. The variance of the different networks for the features 'height' and 'weight' are highest.

input as a weighted pointer to already stored input data, i.e. memories, thereby combining the two hallmarks of hippocampal processing: declarative memory and navigation. The successor representation might therefore be a tool which can be used to navigate through arbitrary cognitive maps, and find similarities in novel inputs as well as past memories.

Furthermore, the discount factor γ of the successor representation can be used to model cognitive maps with different scales, which range in our example from clusters of taxonomic animal classes to individual animal species. The varying grid cell scaling along the long axis of the entorhinal cortex is known to be associated with hierarchical memory content [15]. The discount factor can be used to model this hierarchical structure. In our experiment the hierarchical scale could be used to interpolate novel feature data in different ways. For example if we want to retrieve general information, a large discount factor resulting in dense clusters, to derive averaged information about the whole cluster, can be used. In contrast, for more detailed information regarding a specific state of the cognitive map, a smaller discount factor is useful.

Since our approach works with a direct feature vector as input, it still requires highly pre-processed data. A future outlook for this model could be to include a deep neural network for feature extraction as pre-processing. For instance, image analysis is already a well established field for deep neural networks. Our model could be used to replace the last output layer of such networks, which usually perform a classification task, and use the feature space embeddings to learn a cognitive map. This extended model could enhance the learning from just classification to understanding which features are present in which image. This could potential lead to more context awareness in neural networks.

As recently suggested, the neuroscience of spatial navigation might be of particular importance for artificial intelligence research [50]. A neural network implementation of hippocampal successor representations, especially, promises advances in both fields. Following the research agenda of Cognitive Computational Neuroscience proposed by Kriegeskorte et al. [51], neuroscience and cognitive science benefit from such models by gaining deeper understanding of brain computations [34, 52, 53]. Conversely, for artificial intelligence and machine learning, neural network-based multi-scale successor representations to learn and process structural knowledge as an example of neuroscience-inspired

artificial intelligence [54–57], might be a further step to overcome the limitations of contemporary deep learning [56–61] and towards human-level artificial general intelligence.

Acknowledgments

This work was funded by the Deutsche Forschungsgemeinschaft (DFG, German Research Foundation): grant KR 5148/2-1 to PK (project number 436456810) and grant SCHI 1482/3-1 (project number 451810794) to AS.

Author contributions

PS performed computer simulations and prepared all figures. PS, AM and PK designed the study. PK and AM supervised the study. PS, AS, AM and PK discussed the results and wrote the manuscript.

Competing interests

The authors declare no competing financial interests.

References

- [1] J. O’Keefe and J. Dostrovsky. The hippocampus as a spatial map. Preliminary evidence from unit activity in the freely-moving rat. *Brain Research*, 34(1):171–175, 1971.
- [2] Russell A Epstein, Eva Zita Patai, Joshua B Julian, and Hugo J Spiers. The cognitive map in humans: spatial navigation and beyond. *Nature neuroscience*, 20(11):1504–1513, 2017.
- [3] Seongmin A Park, Douglas S Miller, and Erie D Boorman. Inferences on a multidimensional social hierarchy use a grid-like code. *bioRxiv*, pages 2020–05, 2021.
- [4] Nathaniel J. Killian and Elizabeth A. Buffalo. Grid cells map the visual world. *Nature Neuroscience*, 21(2), 2018.
- [5] Bertram Opitz. Memory function and the hippocampus. *Frontiers of Neurology and Neuroscience*, 34:51–59, 2014.
- [6] Torkel Hafting, Marianne Fyhn, Sturla Molden, May-Britt Moser, and Edvard I Moser. Microstructure of a spatial map in the entorhinal cortex. *Nature*, 436(7052):801–806, 2005.
- [7] John O’Keefe and Jonathan Dostrovsky. The hippocampus as a spatial map: preliminary evidence from unit activity in the freely-moving rat. *Brain research*, 1971.
- [8] John O’keefe and Lynn Nadel. *The hippocampus as a cognitive map*. Oxford university press, 1978.
- [9] Edvard I Moser, May-Britt Moser, and Bruce L McNaughton. Spatial representation in the hippocampal formation: a history. *Nature neuroscience*, 20(11):1448–1464, 2017.
- [10] Eric R. Kandel, editor. *Principles of neural science*. McGraw-Hill, New York, 5th ed edition, 2013.
- [11] Endel Tulving and Hans J Markowitsch. Episodic and declarative memory: role of the hippocampus. *Hippocampus*, 8(3):198–204, 1998.

- [12] Leila Reddy, Benedikt Zoefel, Jessy K Possel, Judith Peters, Doris E Dijksterhuis, Marlene Poncet, Elisabeth CW van Straaten, Johannes C Baayen, Sander Idema, and Matthew W Self. Human hippocampal neurons track moments in a sequence of events. *Journal of Neuroscience*, 41(31):6714–6725, 2021.
- [13] V. I. Kryukov. The role of the hippocampus in long-term memory: is it memory store or comparator? *Journal of Integrative Neuroscience*, 07:117–184, 2008.
- [14] Lynn Nadel and Morris Moscovitch. Memory consolidation, retrograde amnesia and the hippocampal complex. *Current Opinion in Neurobiology*, 7:217–227, 1997.
- [15] Silvy HP Collin, Branka Milivojevic, and Christian F Doeller. Memory hierarchies map onto the hippocampal long axis in humans. *Nature neuroscience*, 18(11):1562–1564, 2015.
- [16] Iva K Brunec and Ida Momennejad. Predictive representations in hippocampal and prefrontal hierarchies. *bioRxiv*, page 786434, 2019.
- [17] Branka Milivojevic and Christian F Doeller. Mnemonic networks in the hippocampal formation: From spatial maps to temporal and conceptual codes. *Journal of Experimental Psychology: General*, 142(4):1231, 2013.
- [18] Ida Momennejad. Learning structures: Predictive representations, replay, and generalization. *Current Opinion in Behavioral Sciences*, 32:155–166, 2020.
- [19] Kimberly L Stachenfeld, Matthew Botvinick, and Samuel J Gershman. Design principles of the hippocampal cognitive map. *Advances in neural information processing systems*, 27:2528–2536, 2014.
- [20] Kimberly L Stachenfeld, Matthew M Botvinick, and Samuel J Gershman. The hippocampus as a predictive map. *Nature neuroscience*, 20(11):1643, 2017.
- [21] Daniel C McNamee, Kimberly L Stachenfeld, Matthew M Botvinick, and Samuel J Gershman. Flexible modulation of sequence generation in the entorhinal–hippocampal system. *Nature neuroscience*, 24(6):851–862, 2021.
- [22] Paul Stoewer, Christian Schlieker, Achim Schilling, Claus Metzner, Andreas Maier, and Patrick Krauss. Neural network based successor representations to form cognitive maps of space and language. *Scientific Reports*, 12:11233, 2022. Number: 1 Publisher: Nature Publishing Group.
- [23] Peter Dayan. Improving Generalization for Temporal Difference Learning: The Successor Representation. *Neural Computation*, 5(4):613–624, 07 1993.
- [24] Laurens Van der Maaten and Geoffrey Hinton. Visualizing data using t-sne. *Journal of machine learning research*, 9(11), 2008.
- [25] Martin Wattenberg, Fernanda Viégas, and Ian Johnson. How to use t-sne effectively. *Distill*, 1(10):e2, 2016.
- [26] Catalina A Vallejos. Exploring a world of a thousand dimensions. *Nature biotechnology*, 37(12):1423–1424, 2019.
- [27] Kevin R Moon, David van Dijk, Zheng Wang, Scott Gigante, Daniel B Burkhardt, William S Chen, Kristina Yim, Antonia van den Elzen, Matthew J Hirn, Ronald R Coifman, et al. Visualizing structure and transitions in high-dimensional biological data. *Nature biotechnology*, 37(12):1482–1492, 2019.

- [28] Warren S Torgerson. Multidimensional scaling: I. theory and method. *Psychometrika*, 17(4):401–419, 1952.
- [29] Joseph B Kruskal. Nonmetric multidimensional scaling: a numerical method. *Psychometrika*, 29(2):115–129, 1964.
- [30] Joseph B Kruskal. *Multidimensional scaling*. Number 11. Sage, 1978.
- [31] Michael AA Cox and Trevor F Cox. Multidimensional scaling. In *Handbook of data visualization*, pages 315–347. Springer, 2008.
- [32] Achim Schilling, Rosario Tomasello, Malte R Henningsen-Schomers, Alexandra Zankl, Kishore Surendra, Martin Haller, Valerie Karl, Peter Uhrig, Andreas Maier, and Patrick Krauss. Analysis of continuous neuronal activity evoked by natural speech with computational corpus linguistics methods. *Language, Cognition and Neuroscience*, 36(2):167–186, 2021.
- [33] Achim Schilling, Andreas Maier, Richard Gerum, Claus Metzner, and Patrick Krauss. Quantifying the separability of data classes in neural networks. *Neural Networks*, 139:278–293, 2021.
- [34] Patrick Krauss, Claus Metzner, Nidhi Joshi, Holger Schulze, Maximilian Traxdorf, Andreas Maier, and Achim Schilling. Analysis and visualization of sleep stages based on deep neural networks. *Neurobiology of sleep and circadian rhythms*, 10:100064, 2021.
- [35] Patrick Krauss, Alexandra Zankl, Achim Schilling, Holger Schulze, and Claus Metzner. Analysis of structure and dynamics in three-neuron motifs. *Frontiers in Computational Neuroscience*, 13:5, 2019.
- [36] Patrick Krauss, Karin Prebeck, Achim Schilling, and Claus Metzner. Recurrence resonance” in three-neuron motifs. *Frontiers in computational neuroscience*, page 64, 2019.
- [37] Patrick Krauss, Marc Schuster, Verena Dietrich, Achim Schilling, Holger Schulze, and Claus Metzner. Weight statistics controls dynamics in recurrent neural networks. *PloS one*, 14(4):e0214541, 2019.
- [38] Patrick Krauss, Claus Metzner, Achim Schilling, Konstantin Tziridis, Maximilian Traxdorf, Andreas Wollbrink, Stefan Rampp, Christo Pantev, and Holger Schulze. A statistical method for analyzing and comparing spatiotemporal cortical activation patterns. *Scientific reports*, 8(1):1–9, 2018.
- [39] Patrick Krauss, Achim Schilling, Judith Bauer, Konstantin Tziridis, Claus Metzner, Holger Schulze, and Maximilian Traxdorf. Analysis of multichannel eeg patterns during human sleep: a novel approach. *Frontiers in human neuroscience*, 12:121, 2018.
- [40] Maximilian Traxdorf, Patrick Krauss, Achim Schilling, Holger Schulze, and Konstantin Tziridis. Microstructure of cortical activity during sleep reflects respiratory events and state of daytime vigilance. *Somnologie*, 23(2):72–79, 2019.
- [41] François Chollet et al. Keras, 2015.
- [42] Martín Abadi, Ashish Agarwal, Paul Barham, Eugene Brevdo, Zhifeng Chen, Craig Citro, Greg S. Corrado, Andy Davis, Jeffrey Dean, Matthieu Devin, Sanjay Ghemawat, Ian Goodfellow, Andrew Harp, Geoffrey Irving, Michael Isard, Yangqing Jia, Rafal Jozefowicz, Lukasz Kaiser, Manjunath Kudlur, Josh Levenberg, Dandelion Mané, Rajat Monga, Sherry Moore, Derek Murray, Chris Olah, Mike Schuster, Jonathon Shlens, Benoit Steiner, Ilya Sutskever, Kunal Talwar, Paul Tucker, Vincent Vanhoucke, Vijay Vasudevan, Fernanda Viégas, Oriol Vinyals, Pete Warden, Martin Wattenberg, Martin Wicke, Yuan Yu, and Xiaoqiang Zheng.

TensorFlow: Large-scale machine learning on heterogeneous systems, 2015. Software available from tensorflow.org.

- [43] Charles R. Harris, K. Jarrod Millman, St'efan J. van der Walt, Ralf Gommers, Pauli Virtanen, David Cournapeau, Eric Wieser, Julian Taylor, Sebastian Berg, Nathaniel J. Smith, Robert Kern, Matti Picus, Stephan Hoyer, Marten H. van Kerkwijk, Matthew Brett, Allan Haldane, Jaime Fern'andez del R'io, Mark Wiebe, Pearu Peterson, Pierre G'erard-Marchant, Kevin Sheppard, Tyler Reddy, Warren Weckesser, Hameer Abbasi, Christoph Gohlke, and Travis E. Oliphant. Array programming with NumPy. *Nature*, 585(7825):357–362, September 2020.
- [44] F. Pedregosa, G. Varoquaux, A. Gramfort, V. Michel, B. Thirion, O. Grisel, M. Blondel, P. Prettenhofer, R. Weiss, V. Dubourg, J. Vanderplas, A. Passos, D. Cournapeau, M. Brucher, M. Perrot, and E. Duchesnay. Scikit-learn: Machine learning in Python. *Journal of Machine Learning Research*, 12:2825–2830, 2011.
- [45] J. D. Hunter. Matplotlib: A 2d graphics environment. *Computing in Science & Engineering*, 9(3):90–95, 2007.
- [46] Teuvo Kohonen. The self-organizing map. *Proceedings of the IEEE*, 78(9):1464–1480, 1990.
- [47] Jean Aitchison. *Words in the mind: An introduction to the mental lexicon*. John Wiley & Sons, 2012.
- [48] D Alan Cruse. Prototype theory and lexical semantics. In *Meanings and Prototypes (RLE Linguistics B: Grammar)*, pages 392–412. Routledge, 2014.
- [49] Jacob LS Bellmund, Peter Gärdenfors, Edvard I Moser, and Christian F Doeller. Navigating cognition: Spatial codes for human thinking. *Science*, 362(6415), 2018.
- [50] Edgar Bermudez-Contreras, Benjamin J Clark, and Aaron Wilber. The neuroscience of spatial navigation and the relationship to artificial intelligence. *Frontiers in Computational Neuroscience*, 14:63, 2020.
- [51] Nikolaus Kriegeskorte and Pamela K Douglas. Cognitive computational neuroscience. *Nature neuroscience*, 21(9):1148–1160, 2018.
- [52] Achim Schilling, Richard Gerum, Alexandra Zankl, Holger Schulze, Claus Metzner, and Patrick Krauss. Intrinsic noise improves speech recognition in a computational model of the auditory pathway. *bioRxiv*, 2020.
- [53] Patrick Krauss, Konstantin Tziridis, Achim Schilling, and Holger Schulze. Cross-modal stochastic resonance as a universal principle to enhance sensory processing. *Frontiers in neuroscience*, 12:578, 2018.
- [54] Demis Hassabis, Dharshan Kumaran, Christopher Summerfield, and Matthew Botvinick. Neuroscience-inspired artificial intelligence. *Neuron*, 95(2):245–258, 2017.
- [55] Patrick Krauss and Andreas Maier. Will we ever have conscious machines? *Frontiers in computational neuroscience*, page 116, 2020.
- [56] Zijin Yang, Achim Schilling, Andreas Maier, and Patrick Krauss. Neural networks with fixed binary random projections improve accuracy in classifying noisy data. In *Bildverarbeitung für die Medizin 2021*, pages 211–216. Springer, 2021.

- [57] Andreas Maier, Harald Köstler, Marco Heisig, Patrick Krauss, and Seung Hee Yang. Known operator learning and hybrid machine learning in medical imaging—a review of the past, the present, and the future. *Progress in Biomedical Engineering*, 2022.
- [58] Patrick Krauss, Claus Metzner, Janina Lange, Nadine Lang, and Ben Fabry. Parameter-free binarization and skeletonization of fiber networks from confocal image stacks. *PLoS One*, 7(5):e36575, 2012.
- [59] Gary Marcus. Deep learning: A critical appraisal. *arXiv preprint arXiv:1801.00631*, 2018.
- [60] Richard C Gerum and Achim Schilling. Integration of leaky-integrate-and-fire neurons in standard machine learning architectures to generate hybrid networks: A surrogate gradient approach. *Neural Computation*, 33(10):2827–2852, 2021.
- [61] Andreas K Maier, Christopher Syben, Bernhard Stimpel, Tobias Würfl, Mathis Hoffmann, Frank Schebesch, Weilin Fu, Leonid Mill, Lasse Kling, and Silke Christiansen. Learning with known operators reduces maximum error bounds. *Nature machine intelligence*, 1(8):373–380, 2019.